Beta-Decay Theory and the Spectrum of Rb^{87}†*

M. A. PRESTON, G. H. KEECH, AND J. M. PEARSON‡
Department of Physics, McMaster University, Hamilton, Ontario, Canada
(Received January 11, 1960)

The shape of the third forbidden β spectrum of Rb^{87} has been analyzed. It has been found to be consistent with (i) a mixture of vector and axial vector interactions, (ii) the same value and sign of the ratio g_A/g_V as found for the neutron, and (iii) a shell model evaluation of the nuclear matrix elements.

INTRODUCTION

THE strong evidence that the nuclear β-decay interaction is a mixture in roughly equal proportions of vector and axial vector terms is based mostly on measurements in allowed transitions of various angular correlations and half-lives. There would seem to be some interest in checking that the spectral shapes of forbidden decays with distorted Kurie plots are consistent with the currently accepted interaction. Moreover, it is in principle possible from an analysis of a forbidden spectrum to determine the coupling constant ratio g_V/g_A and it is of interest to see if there is any indication of this ratio changing with nuclide or with order of forbiddenness. In order to accomplish this last objective it is necessary to have an estimate of the nuclear matrix elements involved. With our present knowledge of nuclear structure, such estimates cannot be very precise, but this uncertainty can be to some extent reduced by a suitable choice of nuclide.

For these reasons the analysis of the decay of Rb^{87} is of some interest. There is a third forbidden transition from the $\frac{3}{2}-$ ground state of Rb^{87} to the $9/2+$ ground state of Sr^{87}. There are no other transitions to mask the low-energy part of the spectrum—as there are for so many forbidden spectra. Moreover Rb^{87} contains 50 neutrons and Sr^{87} contains 38 protons, completing the $(2p_{\frac{3}{2}}, 1f_{\frac{5}{2}})$ subshell. Consequently one may hope that simple nuclear wave functions will be more reliable than usual.

This transition with $\Delta J=3$ and parity change has an allowed Fermi-Kurie plot with considerable curvature which makes the analysis for g_V/g_A possible. The data used for the spectrum were obtained by Goodman.[1] In these experiments special steps were taken to minimize the effects of source thickness and of background counting rates. It is believed that these data are the most accurate available particularly at the low-energy end of the spectrum. We made our own reduction of the raw data to obtain a counting rate $n(E)$. The results are very similar to those obtained by MacGregor and Wiedenbeck.[2] The allowed Fermi-Kurie plot of Goodman's data as analyzed by us is compared with that of MacGregor and Wiedenbeck in Fig. 1. Goodman's data lead to an end point of 280 ± 5 kev. We have used three end points, 275, 280, and 285 kev, in order to examine the effect on the results of varying this parameter.

ANALYSIS OF THE SPECTRUM

The counting rate for a $\Delta J=3$, yes transition is

$$n(E)dE=(2\pi)^{-3}pE(W-E)^2FC_3dE \qquad (1)$$

where as usual, $m=\hbar=c=1$, p, E and W are, respectively, the electron momentum, electron energy and end point, and F is the Fermi function. We assume that the β-decay interaction is a mixture of vector and axial vector interactions and normalize the coupling constants so that the vector interaction, for example, is

$$\Psi^*\gamma_4\gamma_\mu\Phi\psi^*\gamma_4\gamma_\mu(g_V+g_V'\gamma_5)\varphi.$$

Then if we assume $g_V'/g_V=g_A'/g_A=r$, we can write

$$\begin{aligned}C_3=(1+r^2)\{&g_V^2|Q_3(\mathbf{r})|^2\sum_{\nu=0}^{3}[A_{3\nu}q^{4-2\nu}M_\nu-2C_{3\nu}q^{5-2\nu}N_\nu\\&+D_{3\nu}q^{6-2\nu}L_\nu]+g_V^2|Q_3(\boldsymbol{\alpha})|^2\sum_{\nu=0}^{2}A_{3\nu}q^{4-2\nu}L_\nu\\&+2g_V^2\,\mathrm{Im}[Q_3(\boldsymbol{\alpha})Q_3^*(\mathbf{r})]\sum_{\nu=0}^{2}[A_{3\nu}q^{4-2\nu}N_\nu-C_{3\nu}q^{5-2\nu}L_\nu]\\&+g_A^2|Q_3(\boldsymbol{\sigma}\times\mathbf{r})|^2\sum_{\nu=0}^{3}[A_{3\nu}q^{4-2\nu}M_\nu+2C_{3\nu}q^{5-2\nu}N_\nu\\&+(D_{3\nu}-B_{3\nu}/4)q^{6-2\nu}L_\nu]+2g_Ag_V\,\mathrm{Re}[Q_3(\boldsymbol{\alpha})Q_3^*(\boldsymbol{\sigma}\times\mathbf{r})]\\&\times\sum_{\nu=0}^{2}[A_{3\nu}q^{4-2\nu}N_\nu+C_{3\nu}q^{5-2\nu}L_\nu]\\&-2g_Ag_V\,\mathrm{Im}[Q_3(\mathbf{r})Q_3^*(\boldsymbol{\sigma}\times\mathbf{r})]\\&\times\sum_{\nu=0}^{3}[A_{3\nu}q^{4-2\nu}M_\nu+(D_{3\nu}-B_{3\nu})q^{6-2\nu}L_\nu]\\&+g_A^2|Q_4(\boldsymbol{\sigma})|^2\sum_{\nu=0}^{3}B_{3\nu}q^{6-2\nu}L_\nu\}. \qquad (2)\end{aligned}$$

In this equation the various symbols have the conven-

† This research was supported by the National Research Council of Canada and the Ontario Research Foundation.
* Based in part on a thesis submitted by G. H. Keech for the M.Sc. degree at McMaster Unitersity.
‡ Now at Western Reserve University, Cleveland, Ohio.
[1] C. D. Goodman, Ph.D. thesis, University of Rochester, 1955 (unpublished).
[2] M. H. MacGregor and M. L. Wiedenbeck, Phys. Rev. **94**, 138 (1954).

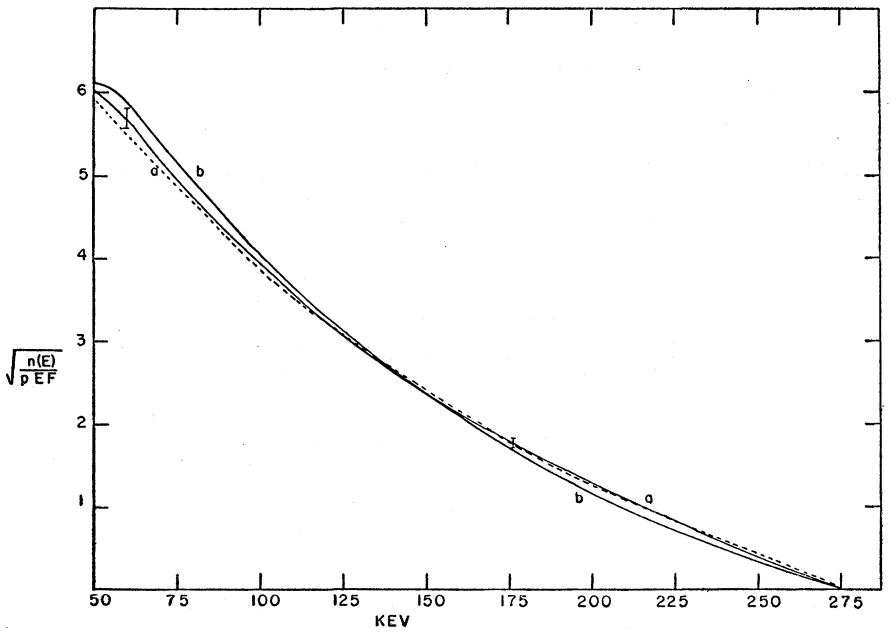

FIG. 1. Allowed Fermi-Kurie plot of the Rb^{87} spectrum. The solid curves (a) and (b) are based respectively on the data of Goodman and of MacGregor and Wiedenbeck. The same end point, 275 kev, is used for both plots. The error markers on curve (a) represent typical limits of the 65% probability zone which we used in constructing the conic bands. The dashed curve is that of Flynn and Glendenin (reference 18) obtained after our analysis was complete. The only noticeable difference from curve (a) is at the lowest energy point we used (60 kev), where the new value is slightly, but not significantly, outside the error limit we assigned.

tional meanings.[3] The Q's are nuclear matrix elements, L_ν, M_ν, and N_ν are functions of the electron momentum, q is the neutrino momentum, and $A_{3\nu}$, $B_{3\nu}$, $C_{3\nu}$, and $D_{3\nu}$ are numerical coefficients. The theorem of Longmire and Messiah[4] shows that the matrix element ratio $Q_{ijk}(\mathbf{A})/Q_{ijk}(\mathbf{B})$ is independent of i, j, k and of the magnetic quantum numbers of the initial and final nuclear states. Consequently, although $Q_3(\mathbf{A})Q_3^*(\mathbf{B})$ stands for $\sum_{i,j,k} Q_{ijk}(\mathbf{A})Q_{ijk}^*(\mathbf{B})$, we can define the real quantities

$$x=\frac{g_V}{g_A}\frac{Q_{ijk}(\mathbf{r})}{Q_{ijk}(\boldsymbol{\sigma}\times\mathbf{r})}, \tag{3a}$$

$$y=\frac{g_V}{g_A}\frac{Q_{ijk}(\boldsymbol{\alpha})}{Q_{ijk}(\boldsymbol{\sigma}\times\mathbf{r})}, \tag{3b}$$

$$u^2=\frac{|Q_4(\boldsymbol{\sigma})|^2}{|Q_3(\boldsymbol{\sigma}\times\mathbf{r})|^2}, \tag{3c}$$

and write Eq. (3) as

$$C_3(p)/(1+r^2)g_A^2|Q_3(\boldsymbol{\sigma}\times\mathbf{r})|^2=Ax^2+By^2-2Dxy+2Gy+2Hx+F+ku^2, \tag{4}$$

where A, B, D, F, G, H, and k are functions of p, whose definitions are obvious by comparison with Eq. (3). In order to avoid difficulties with the absolute value of the counting rate per atom, we have calculated the ratio of the correction factor at each electron momentum to that at a fixed momentum $p_0(=0.8)$ and defining

$$\rho(p)=C_3(p)/C_3(p_0), \tag{5}$$

we obtain for each momentum p the equation

$$A'x^2+B'y^2-2D'xy+2G'y+2H'x+F'+k'u^2=0 \tag{6}$$

where

$$A'(p)=A(p)-\rho(p)A(p_0), \quad \text{etc.}$$

The quantity u^2 is of order of magnitude unity, but fortunately the coefficient $k'\ll F'$, so that the uncertainty in the value of u^2 is not important. Calculations have been made with $u^2=0$ and 2 and there is no appreciable difference between them.

Ignoring u, or fixing its value, Eq. (6) represents a set of conics in x and y, one for each value of p. In principle, an exact solution for x and y could be determined by obtaining the common point of intersection of a few conics of this set. However, experimental error, reflected in a statistical distribution of values for ρ, requires the replacement of each one of these conics by a band of finite width. For each momentum used we have obtained from the experimental data the two extreme values of ρ, symmetric about the mean value, such that there is a 65% probability that the true value lies between them. The two conics corresponding to these two values define a band in the x-y plane. There is such a band for each momentum. There is a high probability that the region of the plane common to all the bands contains the true values (x,y). This conclusion is reinforced by the observation that the bands were made only slightly broader when we took them as 80% rather than 65% zones.

The coefficients A', B', etc., of the conics depend on the functions L_ν, M_ν, N_ν which in turn depend on the

[3] As summarized for example by M. Deutsch and O. Kofoed-Hansen, in *Experimental Nuclear Physics*, edited by E. Segrè (John Wiley and Sons, Inc., New York, 1959), Vol. 3, pp. 517–525. We have written $Q_n(\mathbf{A})$ for $Q_n(\mathbf{A},\mathbf{r})/n!$.

[4] C. L. Longmire and A. M. L. Messiah, Phys. Rev. **83**, 464 (1951).

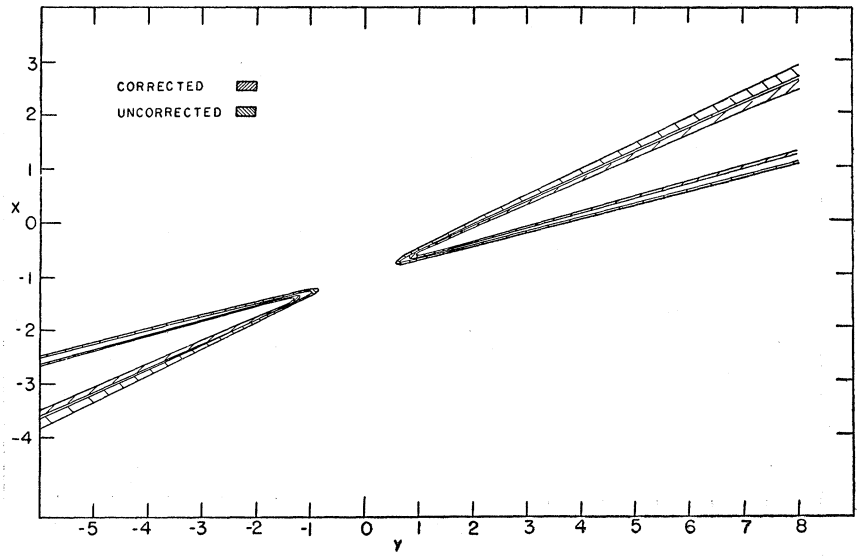

FIG. 2. Conic bands defining allowed values of x and y for $p=0.5$, both corrected and uncorrected for finite nuclear size. The end point used was 275 kev and $R=1.41A^{\frac{1}{3}}\times10^{-13}$ cm.

end point of the spectrum, the effective radius R at which the lepton wave functions are evaluated and the electrostatic potential which determines the form of the electron wave function. The electron wave function should of course be that for a finite nucleus. However, the variation in the results due to changes in the effective β-decay radius R is much greater than the variation due to the change from the point-charge wave function to the finite-nucleus wave function. The effect of the finite-size correction is shown in Fig. 2 which shows the conic bands, for a certain electron momentum, corrected for finite size and not so corrected. The finite-size correction factors for $Z=38$ were approximated from the graphs in the report by Rose and Holmes.[5]

Because of fairly heavy cancellation arising in the calculation of the conics, it was decided to obtain L_ν, M_ν, and N_ν to five figures rather than the four which are tabulated. This was done by taking a further term in the series expansion. The three end-point energies 275, 280, and 285 kev were considered, and the dependence upon the effective radial position R was investigated by considering the three radii 1.13, 1.41, and $1.55A^{\frac{1}{3}}\times10^{-13}$ cm.

In the cases studied, the conics, which serve as boundary curves for the bands of allowed x and y, are all hyperbola of a similar character. For each case, the conic-bands for different momenta differ by only small amounts. Their common area, when this exists, occurs all along one arm of the hyperbolas defining almost a linear relationship for x and y (e.g., Fig. 3). There is

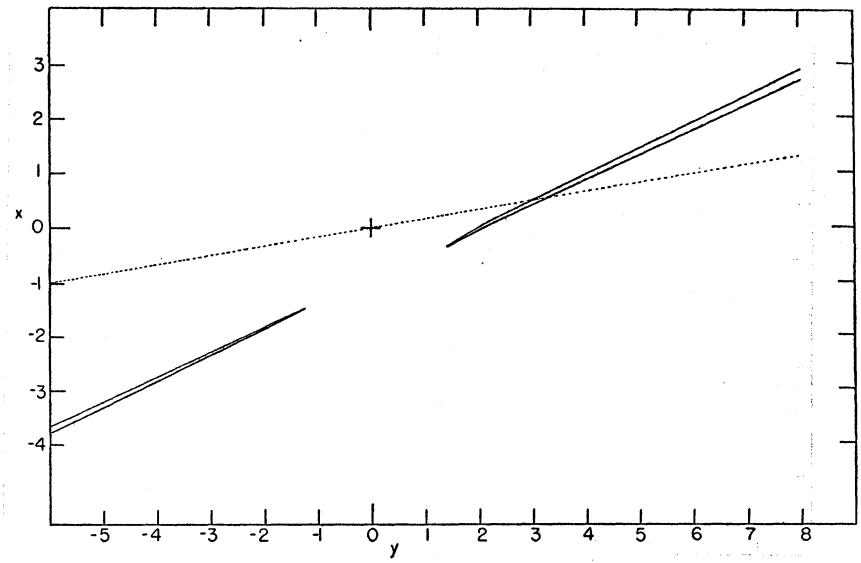

FIG. 3. Allowed regions of the parameters x and y. Any point in the narrow bands shown gives a fit to the observed spectrum shape, if one takes 275 kev for the end point and $1.41A^{\frac{1}{3}}\times10^{-13}$ cm as the effective radius. The line $y=6x$ is shown.

[5] M. E. Rose and D. K. Holmes, Oak Ridge National Laboratory Report 1022 (unpublished); and Phys. Rev. 83, 190 (1951).

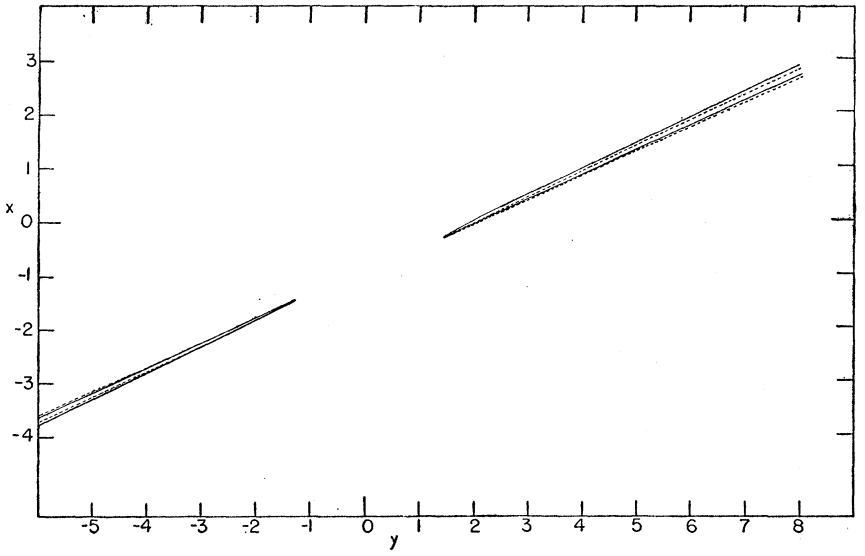

FIG. 4. The allowed regions are shown to change very little with end point. The curves are for $R=1.41A^{\frac{1}{3}}\times10^{-13}$ cm and end points 275 kev and 280 kev.

very little dependence of this area upon the end point chosen (e.g., Fig. 4). The effect of the term containing u^2 is smaller yet, and it can be neglected.

The influence of the effective radius R upon the system of conic bands is appreciable. This is illustrated by the systems for $R=1.13$ and $1.41A^{\frac{1}{3}}\times10^{-13}$ cm (see Figs. 3 and 5). The structures of the common areas are similar, but their positions are shifted somewhat. It is clear that the variation of R has much greater effect than the finite nucleus correction and one may consider that any reasonable electron wave function would give results intermediate to these two figures. The case $R=1.55A^{\frac{1}{3}}\times10^{-13}$ cm does not give any allowed areas. This is not unexpected for such a radial position is well out into the mass distribution tail of the nucleus. Although the variation of the common area with R, as indicated by Figs. 3 and 5, produces small changes in the values of x and y obtained, the important results remain unchanged.

The existence of the common regions makes it plain that the spectrum shape can be fitted with a V, A interaction. We now proceed to see what can be said about the values of g_V and g_A.

MATRIX ELEMENT RATIOS

The analysis of the spectrum indicates acceptable values of the two ratios $x=i(g_V/g_A)Q_3(\mathbf{r})/Q_3(\boldsymbol{\sigma}\times\mathbf{r})$ and $y=(g_V/g_A)Q_3(\boldsymbol{\alpha})/Q_3(\boldsymbol{\sigma}\times\mathbf{r})$. In order to use these results to obtain information about the coupling constants, it is necessary to evaluate the nuclear matrix element ratios. The ratio involved in x has the special property that in the simple shell model its value depends only on the

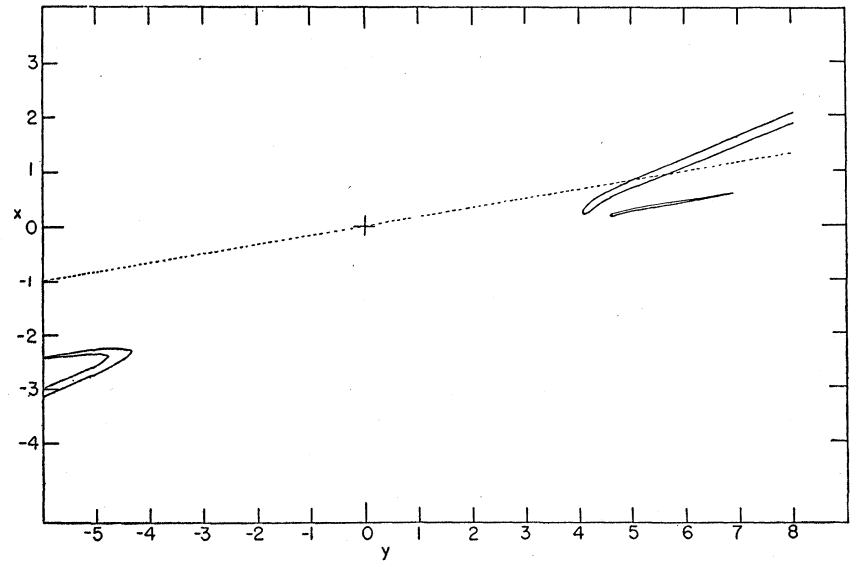

FIG. 5. The allowed regions for $R=1.13A^{\frac{1}{3}}\times10^{-13}$ cm. The line $y=6x$ is shown. The end point used is 280 kev.

angular momenta of the initial and final states and not at all on the radial wave functions, which are much less reliable. The other ratio which we choose to calculate $Q_3(\boldsymbol{\alpha})/Q_3(\mathbf{r})$ gives the ratio y/x which is independent of the coupling constants; its value, however, depends on the radial wave functions.

The energy level scheme of the extreme single-particle model[6] predicts our beta-decay process to be the transition of a $1g_{9/2}$ neutron into a $2p_{\frac{3}{2}}$ proton. This event leaves a hole in the $1g_{9/2}$ neutron level and fills up the $2p_{\frac{3}{2}}$ proton level of Sr^{87}. The measured ground-state spins of Rb^{87} and Sr^{87} are $\frac{3}{2}$ and 9/2, respectively. The measured magnetic moments of Rb^{87} and Sr^{87} lie fairly close to their respective Schmidt "$j=l+\frac{1}{2}$" limits, indicating good agreement with the parity assignments of the extreme single-particle model.[7]

We proceed, therefore, to use the simple shell model to calculate the matrix element ratios. We note, moreover, that configuration mixing is not likely to affect our results. In Rb^{87}, it is reasonable to assume that the 50 neutron structure is common to all configurations in the ground state, that is, that admixed configurations differ from the shell model function only in the proton states. Similarly in Sr^{87}, we assume that all the configurations mixed to make up the ground state have the same filled proton shells, differing only in neutron states. If one now recalls that the β-decay operators are single-particle operators, one sees that the only configurations which can contribute to the β decay are the simple shell model ones. If these are not 100% of the ground state the absolute value of a matrix element is reduced, but the ratio of two matrix elements is not affected.

It is consequently reasonable to assume that for this particular decay, the principal uncertainty in the matrix element ratios lies in the radial wave functions assumed; consequently, the value of x, which is independent of these functions, should be quite good. It is

$$x=-g_V/g_A. \tag{7}$$

To evaluate y/x, we use the result of Longmire and Messiah,[4] and simply calculate

$$\frac{Q_{zzz}(\boldsymbol{\alpha})}{Q_{zzz}(\mathbf{r})}=\frac{\int d\tau\psi_f^*(2p_{\frac{3}{2}})O_{zzz}(\boldsymbol{\alpha})\psi_i(1g_{9/2})}{\int d\tau\psi_f^*(2p_{\frac{3}{2}})O_{zzz}(\mathbf{r})\psi_i(1g_{9/2})}. \tag{8}$$

The operator $O_{zzz}(\mathbf{r})$ is easily written in terms of the spherical harmonics Y_l^m used by Condon and Shortley.[8]

$$O_{zzz}(\mathbf{r})=(4\pi/7)^{\frac{1}{2}}\tfrac{2}{5}r^3Y_3^0.$$

The procedure for the operator $O_{zzz}(\boldsymbol{\alpha})$ is more involved. The odd Dirac operator $\boldsymbol{\alpha}$ is replaced[9] by the even operator $-\mathbf{P}/M$. $\mathbf{P}$ and M are the nucleon momentum and mass, respectively. One finds

$$O_{zzz}(\boldsymbol{\alpha})=\frac{4i}{5M}\left(\frac{\pi}{21}\right)^{\frac{1}{2}}\left(\sqrt{3}Y_3^0r^2\frac{\partial}{\partial r}-Y_3^{-1}rL_+-Y_3^1rL_-\right).$$

Here L_+ and L_- are the angular momentum ladder operators, $L_x\pm iL_y$.

The ratio reduces to

$$\frac{Q_{zzz}(\boldsymbol{\alpha})}{Q_{zzz}(\mathbf{r})}=\frac{i}{M}\frac{\int_0^\infty R_{2p}\left(\frac{dR_{1g}}{dr}\right)r^4dr+5\int_0^\infty R_{2p}R_{1g}r^3dr}{\int_0^\infty R_{2p}R_{1g}r^5dr}. \tag{9}$$

For this type of calculation, the spherical harmonic oscillator radial wave functions should give a fair approximation. Using the results given by Mayer and Jensen,[10] we find

$$Q_{zzz}(\boldsymbol{\alpha})/Q_{zzz}(\mathbf{r})=\tfrac{2}{3}i(\gamma/M). \tag{10}$$

The constant γ is fixed[10] by computing the root mean square radius.

$$\langle r^2\rangle_{nl}=(1/2\gamma)[2(n-1)+l+\tfrac{3}{2}]. \tag{11}$$

Using Hofstadter's value[11]

$$(\langle r^2\rangle_{\mathrm{av}})^{\frac{1}{2}}=(3/5)^{\frac{1}{2}}1.20(87)^{\frac{1}{3}}\times10^{-13}\text{ cm}$$
$$=1.06\times10^{-2}\text{ relativitic unit.} \tag{12}$$

Averaging (11) over the protons of Rb^{87}

$$\langle r^2\rangle_{\mathrm{av}}=1.84/\gamma.$$

Then we have[12]

$$Q_{zzz}(\boldsymbol{\alpha})/Q_{zzz}(\mathbf{r})\simeq6.0i. \tag{13}$$

Yamada[13] has calculated this matrix ratio using the method of Ahrens and Feenberg.[14] Adjusting his value to correspond to our choice of nuclear radius, we obtain

$$Q_{zzz}(\boldsymbol{\alpha})/Q_{zzz}(\mathbf{r})\simeq2.8i. \tag{14}$$

These results agree in sign, and the disagreement in absolute values is not unreasonable, since the value (14) is based on the semiempirical mass formula and is of general application, whereas the value (13) is obtained by a calculation more specific to one nucleus. The shell

[6] J. P. Elliot and A. M. Lane, *Handbuch der Physik*, edited by S. Flügge (Springer-Verlag, Berlin, 1957), Vol. 39.
[7] R. J. Blin-Stoyle, *Theories of Nuclear Moments* (Oxford University Press, New York, 1957).
[8] E. U. Condon and G. H. Shortley, *Theory of Atomic Spectra* (Cambridge University Press, New York, 1935).
[9] M. E. Rose and R. K. Osborn, Phys. Rev. **93**, 1315 (1954).
[10] M. G. Mayer and J. H. D. Jensen, *The Elementary Theory of Shell Structure* (John Wiley & Sons, New York, 1955).
[11] R. Hofstadter, Revs. Modern Phys. **28**, 214 (1956).
[12] This result may also be obtained by using spherical, rather than Cartesian, tensors. In checking our calculation by this method, we detected a misprint in Eq. (19) of the paper by M. E. Rose and R. K. Osborn, Phys. Rev. **93**, 1326 (1956), viz., the power of -1 in the phase should be $l'+j-\frac{1}{2}$ and *not* $l'+j'-\frac{1}{2}$.
[13] M. Yamada, Progr. Theoret. Phys. (Kyoto) **9**, 268 (1953).
[14] T. Ahrens and E. Feenberg, Phys. Rev. **86**, 64 (1952).

model value $6.0i$ may be more reliable in the special case of Rb^{87}.

RESULTS

Equation (13) gives $y=6x$. This line is plotted in Figs. 3 and 5 to show its intersection with the allowed areas of x and y values found in the conic analysis. In Fig. 3 with $R=1.41A^{\frac{1}{3}}\times10^{-13}$ cm, the intersection gives for x the values between 0.53 and 0.58, while for $R=1.13A^{\frac{1}{3}}\times10^{-13}$ cm the corresponding values are 0.83 and 0.93 (Fig. 5). Intermediate values of R will give intermediate ranges of x values. The quantity x is close to $-g_V/g_A$. The values of $-g_V/g_A$ found directly are

(i) from the decay of polarized neutrons[15]: $-g_V/g_A=0.80\pm0.03$;

(ii) from the lifetimes of O^{14} and of the neutron[16]: $|g_V/g_A|=0.84\pm0.03$.

The last value assumes that g_V is the same for the neutron and for O^{14}. Recent theories[17] suggest that g_V should be independent of any renormalization due to strong interactions and hence should be the same for all nuclides. If the same were true for g_A we might use the above result to argue that the smaller effective radius R is the better one to use. The smaller value is also favored on other grounds. However, there is no reason to assume g_A is constant; we merely note that this assumption is consistent with our results, but so is some variation.

Since our matrix element calculation assumed a specific nuclear model, we cannot insist on the value 6 for y/x, although it should be recalled that the simplest forms of configuration mixing do not change this value. If y/x is increased, the allowed values of x become less but remain positive; if y/x is decreased, x increases, remaining positive, until y/x reaches about 2, when large negative x values appear. If with the restriction that y/x be not more than a factor of three or four different from the calculated value, we couple the further restriction that $|x|\lesssim1$, we can definitely conclude that x is positive and g_V/g_A negative (see Figs. 3 and 5).

As we have already remarked, the uncertainties in the nuclear matrix elements prevent one from using these results to test possible dependence of g_V/g_A on nuclear size. It is, however, interesting to remark that if we take the average value for light nuclides, $g_V/g_A=-0.82$, we find that for $R=1.41A^{\frac{1}{3}}\times10^{-13}$ cm, the point on the conic is $y=3.8$ and for $R=1.13A^{\frac{1}{3}}\times10^{-13}$ cm, $y=5.2$. These values correspond to $y/x=4.7$ and 6.3, in good agreement with the "theoretical" value 6.0.

As a further check of the consistency of our assignments of values for coupling constants and matrix elements, we have calculated the half-life of the transition. We have taken $g_V/g_A=-0.82$, $y=6x=4.92$ and $g_V=2.85\times10^{-12}$, the value appropriate to O^{14}. We have also used the 280-kev end point and a radius in the correction factor of $1.13A^{\frac{1}{3}}\times10^{-13}$ cm. With a half-life 4.7×10^{10} yr,[18] one finds the "experimental" value $Q_3(\mathbf{r})=1.5\times10^{-7}$. On the other hand, we may use the oscillator wave functions to obtain a calculated value, just as we did for the ratio $Q_3(\boldsymbol{\alpha})/Q_3(\mathbf{r})$. This result is $Q_3(\mathbf{r})=5.5\times10^{-7}$. The shell model and experimental results differ, therefore, by a factor of about four, or more precisely the experimental value of the square of the matrix element is about 1/13 of the calculated shell model value. It will be recalled that we pointed out that although configuration mixing would not affect our ratios x and y, it would affect the absolute value of the matrix elements. For unfavored allowed transitions in the same region of the periodic table, the experimental matrix elements are 1/10 to 1/50 of the shell model values. Consequently we are satisfied that our interpretation of the data is self consistent.

[15] M. T. Burgy, V. E. Krohn, T. B. Novey, G. R. Ringo, and V. L. Telegdi, Phys. Rev. **110**, 1214 (1958).

[16] A. N. Sosnovskij, P. E. Spivak, Yu. A. Prokofiev, I. E. Kutikov, and Yu. P. Dobrynin, *Proceedings of the 1958 International Conference on High-Energy Physics at CERN*, edited by B. Ferretti (CERN Scientific Information Service, Geneva, 1958), p. 237; J. B. Gerhart, Phys. Rev. **109**, 897 (1958).

[17] R. P. Feynman and M. Gell-Mann, Phys. Rev. **109**, 193 (1958).

[18] K. F. Flynn and L. E. Glendenin, Phys. Rev. **116**, 744 (1959).